Ignition front structure in a methane-air jet.[1]

J.Ray[2], H. N. Najm and R. B. McCoy
Sandia National Laboratories, Livermore, CA 94551-0969
{jairay, hnnajm, rbmccoy}@ca.sandia.gov

March 21^{st}, 2001

Abstract

We present results from computations of an igniting non-premixed methane jet in coflow air using the GRImech1.2 chemical mechanism. Ignition is initiated in the jet mixing layer with the application of a short-duration heat-flux pulse along a narrow strip. An ignition kernel is formed in the rich mixture region inside the jet and is observed to propagate towards the stoichiometric mixture fraction line in the mixing layer. As the kernel penetrates the stoichiometric region, we observe the formation of a thin circular flame front which burns through the mixing layer and extinguishes at the lean edge. This leaves two edge-flames propagating away from this location along the stoichiometric line. We analyze the reaction zone internal structure and the chemical pathways in the flame fronts during the entire process, comparing them to those of 1D premixed flames at similar stoichiometries, and to results from earlier edge-flame studies. The fronts are seen to move at speeds 2-3 times that of the corresponding premixed flame, as they burn through preheated premixed radicals on the edge of the ignition zone. The strength of the front propagating away from the ignition zone is seen to decay gradually as it encounters lower-temperature gases with diminished availability of radicals.

[1]Presented at the 2^{nd} Joint Meeting of the U.S. Section of the Combustion Institute, Oakland, CA. March 25^{th} to 28^{th}, 2001

[2]Corresponding Author

1 Introduction

Auto-ignition in turbulent non- or partially premixed environments [1] and flame spread give rise to situations where flames ignite and propagate through regions with stratified fuel concentration fields. Such phenomena have been extensively studied in simplified settings, as in the contexts of lifted laminar jet flames [2, 3] and flame propagation in two-dimensional mixing layers [4, 5, 6]. Tribrachial or triple flames have been observed in both the cases, and have been studied as a possible mechanism for the stabilization of lifted flames [7, 2].

Tribrachial flames consist of a diffusion flame aligned and centered on (approximately) the stoichiometric line and terminated by a premixed flame which ranges from the rich to the lean side of the mixture. The diffusion flame is stabilized at the triple point (the locus of the lean and rich premixed flames and the diffusion flame) and is fed by the "excess"/unconsumed fuel and oxidizer on either side of the stoichiometric line. The effect of complex chemistry and transport on such triple flames have been studied by Plessing et al. [8]. Triple flames are inherently asymmetric (because of the asymmetry of flammability limits, reacting mixture composition and burning rates); further, the diffusion flame is usually fed by stable molecules like CO and H_2 since very little of the original fuel survives beyond the premixed fronts.

The triple flame is a region of intense production/consumption and gradients of radicals like OH, H and O, which also diffuse at very different rates. This along with thermal diffusivity makes for substantial differential diffusion effects [6]. Further, the premixed fronts in a triple flame are curved, which focus the diffusion of certain radicals into a small region, enhancing the burning and propagation rates of a triple flame, as compared to a stoichiometric premixed flame.

In this study we ignite a methane-air jet and track the evolution of the ignition front into triple flame-like objects. We study the edge flame as it relaxes after ignition with respect to its structure and identify the dominant reactions. It is seen that C_1 chemistry is dominant in the ignition front and the diffusion flame is fed by CO and H_2 rather than methane. Also, a two-layered radical production region, common in many premixed hydrocarbon flames, is seen in the ignition front.

2 Problem Description

2.1 Physical Description

The physical system being simulated is a 2D CH_4 jet (inlet velocity of 0.8 m/s) with coflow air at 0.25 m/s. The methane is diluted 40 % (by volume) with N_2. The domain in 10 cm $\times$ 5 cm in

size and the jet is 4 cm wide. A spark (heat source) is ignited 1.0 cm above the jet inlet and has a duration of 1 ms.

2.2 Simulation Details

A DNS simulation is done of the igniting jet. GRImech 1.2 is used as the chemical mechanism. Binary diffusion into N_2 is used since the system is N_2 diluted. Adaptive mesh refinement (AMR) is used to preserve resolution. The coarsest mesh cell has a size of 1.25 mm and the finest 19 microns.

Details of the numerical method are in [7, 9, 10]. Briefly, a low Mach number formulation of the Navier-Stokes equation is used. Second-order upwind Godunov is used for spatial discretization. Time integration is done in an operator-split manner. The convective and diffusion operators in the scalar equations (temperature and species) are integrated using a second-order Runge-Kutta scheme while the chemical source term is integrated using a stiff integrator [11, 12]. Sandwiching a stiff integration of Δt between 2 RK2 integrations of $\Delta t/2$ each, gives, by Strang splitting, a formal second-order accuracy. The momentum equations are solved via a vortex method. The 2D momentum equations are cast into the vorticity evolution form. The circulation generated in a given region (usually a cell on a fine, though not necessarily finest mesh level) by the baroclinic and viscous terms is evaluated on the AMR (Eulerian) mesh and injected into the flow-field as a Gaussian vortex particle. The same approach is adopted for the divergence equation, except that expansion particles are injected. The velocity field induced by these particles is calculated using the Fast Multipole Method [13]. Boundary conditions (smooth coflow on the sides, inflow and outflow) are imposed using a potential panel method.

The flowfield is initialized with a parallel streams of air and CH_4 and then allowed to relax into a steady jet. Heating (for ignition) is started after all time derivatives become very small. A second case, with coflow faster than the jet (coflow 0.8 m/s, jet 0.25 m/s) was also simulated to investigate flame structure when the strain rate field was reversed.

3 Ignition Details

In Fig. 1 we show the heat release rates plotted at 3 different time instants to show the progression of the ignition. The contours are of Z where

$$Z = \frac{1}{2}\left(1 + \frac{\nu_{ox}}{\nu_f} X_f - X_{ox}\right)$$

where subscripts ox and f stand for oxidizer (O_2) and fuel (CH_4) and ν is the stoichiometric coefficient. The second black contour represents the stoichiometric line (Z = 0.5). The ignition fronts traverse a vertical distance of approximately 1 cm (the domain shown in the figure) in about 2 ms. The last picture shows the mesh at the last time instant and is seen to be concentrated at the ignition fronts. We see that the premixed "wings" extend from the rich to lean side of the mixing layer. In Fig. 2 we plot the consumption rate of CH_4 in the lower ignition front. The black line is the stoichiometric mixture fraction contour [14]. The graph shows production rate as sampled along the black line and is a measure of the resolution of the structure by the mesh. The sample points are plotted with symbols.

In Fig. 3 (a) we plot the heat release rate along the stoichiometric line for different times. The peak heat release is seen to relax though the heat release rate is about an order of magnitude higher than in a 1D premixed flame of similar N_2 dilution. Further, the front velocity, estimated from the peaks of the heat release rate graph between t = 3.55 ms and 4.15 ms is about 120 cm/s, about 4 times higher than that of a 1D premixed flame. In Fig. 3 (b) we plot the mole fraction of OH. We see that a build up of OH from the heating/early ignition phase is left over and is expected to affect the reactions that occur in the premixed kernel.

In Fig. 4 we plot the mole fractions of OH and CO in the lower left ignition front. We see that the "tongue"-shaped OH pool is bordered on the rich side (the black line is the stoichiometric mixture fraction line [14]) by a pool of CO which also curves around the leading edge of the flame. Most of the OH actually resides far downstream of the lower ignition front, an outcome of the early ignition phase as well as the slow recombination reactions affecting OH. In Fig. 5 we compare this topology with experimental images of the OH and CO concentrations at the base of a lifted methane jet [15]; they are qualitatively similar.

In Fig. 6, we plot mole fractions of CH_4, O_2, CO, H_2, O and OH at the lower left ignition front. Methane is almost entirely consumed at the premixed flame kernel, though O_2 wraps around it. The oxidation at t = 5.35 ms proceeds mainly down the C_1 chain $CH_4 \rightarrow CH_3 \rightarrow CH_2O \rightarrow HCO \rightarrow CO \rightarrow CO_2$. Some of the CH_3 also flows via $CH_3 \rightarrow CH_2(S) \rightarrow CH_2 \rightarrow HCO$. Most of the oxidation into HCO occurs in the premixed kernel while the others are more distributed. HCO is consumed mostly by its decomposition into CO

$$HCO + H_2O \rightleftharpoons H + CO + H_2.$$

Behind the premixed kernel, the diffusion flame is fueled mainly by CO and H_2 (which are formed by the reaction of hydrocarbon intermediates with H and OH) diffusing in from the rich side and

OH and O from the lean side. The black line is the stoichiometric mixture fraction contour. These results are similar to those in [6] where they observe a methanol-air triple flame in a mixing layer.

Reactions involving O are more intense on the lean side and along the stoichiometric line. It is formed by the chain branching reaction

$$\mathrm{H} + \mathrm{O}_2 \rightleftharpoons \mathrm{O} + \mathrm{OH}$$

and consumed by the reactions

$$\mathrm{O} + \mathrm{CH}_3 \rightleftharpoons \mathrm{H} + \mathrm{CH}_2\mathrm{O}$$

and

$$\mathrm{O} + \mathrm{H}_2 \rightleftharpoons \mathrm{H} + \mathrm{OH}.$$

H is formed by interactions of O or OH with hydrocarbons (HCO, CO, CH_3) or H_2 and consumed by O_2 (the chain-branching reaction above) or CH_4 (to give CH_3). These reactions are concentrated around the premixed kernel or on the rich side where hydrocarbon radicals or H_2 (formed by the breakup of methane or CH_2O in the presence of H) can be found. H, O and OH are formed at the trailing edge of the premixed front and diffuse out to attack the incoming fuel and oxidizer at the leading edge. H_2, formed by the breakup of methane at the leading edge diffuses in and is focussed in by the curved ignition front, increasing the concentration of H_2 near the center of curvature. H_2 is consumed by

$$\mathrm{OH} + \mathrm{H}_2 \rightleftharpoons \mathrm{H}_2\mathrm{O} + \mathrm{H}$$

and

$$\mathrm{O} + \mathrm{H}_2 \rightleftharpoons \mathrm{H} + \mathrm{OH},$$

another chain-branching reaction. The focusing thus creates a surfeit of radicals and enhances the rate of burning, as compared to a 1D premixed flame.

In Fig. 7, on the left, we plot the contribution of each of the reactions (in GRImech 1.2) to the heat released in the premixed kernel, as circumscribed by a heat release contour of 30 cal/cm^{2}s. On the right we plot the average mole fractions of species in the same region. The plots of mole fractions show some presence of C_2 compounds. The reactions contributing to the heat release rate are similar to those in a 1D premixed flame and in roughly the same proportions. The absolute contributions, however, are larger than in a 1D premixed flame since the ignition front is a very fast burning flame at the time instant analysed. The main reactions are R10, R38, R52, R84, R99, R101 and R135 which are, respectively,

$$\mathrm{O} + \mathrm{CH}_3 \rightleftharpoons \mathrm{H} + \mathrm{CH2O}$$

$$\mathrm{H} + \mathrm{O_2} \rightleftharpoons \mathrm{O} + \mathrm{OH}$$

$$\mathrm{H} + \mathrm{CH_3}(+\mathrm{M}) \rightleftharpoons \mathrm{CH_4}(+\mathrm{M})$$

$$\mathrm{OH} + \mathrm{H_2} \rightleftharpoons \mathrm{H} + \mathrm{H_2O}$$

$$\mathrm{OH} + \mathrm{CO} \rightleftharpoons \mathrm{H} + \mathrm{CO_2}$$

$$\mathrm{OH} + \mathrm{CH_2O} \rightleftharpoons \mathrm{HCO} + \mathrm{H_2O}$$

$$\mathrm{CH_2} + \mathrm{O_2} \rightleftharpoons \mathrm{OH} + \mathrm{HCO}$$

In Fig. 8 we compare the development of the ignition fronts (depicted via the production rate of H_2O) for the case where the strain rate field is reversed (i.e the coflow is 0.8 m/s and the methane jet is 0.25 m/s). We see that the development is very similar, indicating that the effect of the reversal of the global strain rate field in the vicinity of the edge flame is insignificant. The lean branch in the second (faster coflow) case is pushed in towards the stoichiometric line. In Fig. 9 we plot the fuel inflow velocity into and strain rate tangential to the ignition front - they are remarkably similar.

4 Conclusions

We have presented results of a CH_4 jet being ignited in coflow air by means of a spark. Ignition fronts propagate along the mixing layer, within flammability limits, relaxing to lower speeds of propagation and heat release in time. These ignition fronts exhibit structures similar to triple flames [6]. We present the contribution to the heat release rate by each of the reactions and the mole fraction of species in the premixed kernel and find some qualitative similarities with a 1D premixed flame.

5 Acknowledgement

This work was supported by the US Department of Energy, Office of Basic Energy Sciences, Chemical Sciences Division. Computations were done on the SGI Origin 2000s in Sandia National Laboratories, Livermore, CA.

References

[1] E. Mastorakos, T. A. Baritaud, and T. J. Poinsot. Numerical simulations of autoignition in turbulent mixing flows. *Combustion and Flame*, 109:198–223, 1997.

[2] B. J. Lee and S. H. Chung. Stabilization of lifted tribrachial flames in laminar non-premixed jets. *Combustion and Flame*, 109:163–172, 1997.

[3] M. S. Cha and S. H. Chung. Characteristics of lifted flames in non-premixed turbulent confined jets. In *Twenty-Sixth Symposium (International) on Combustion*, pages 121–128. The Combustion Institute, 1996.

[4] H. G. Im, J. H. Chen, and C. K. Law. Ignition of hydrogen-air mixing layer in turbulent flows. In *Twenty-Seventh Symposium (International) on Combustion*, pages 1047–1056. The Combustion Institute, 1998.

[5] H. G. Im and J. H. Chen. Structure and propagation of triple flames in partially premixed hydrogen-air mixtures. *Combustion and Flame*, 119:436–454, 1999.

[6] T. Echekki and Jacqueline H. Chen. Structure and propagation of methanol-air triple flames. *Combustion and Flame*, 114:231–245, 1998.

[7] J. Ray, H. N. Najm, R. B. Milne, K. D. Devine, and S. Kempka. Triple flame structure and dynamics at the stabilization point of an unsteady lifted jet diffusion flame. *Proc. Combust. Inst.*, 2000. To be published.

[8] T. Plessing, P. Terhoeven, N. Peters, and M. Mansour. An experimental and numerical study of a laminar triple flame. *Combustion and Flame*, 115:335–353, 1998.

[9] H.N. Najm, R.B. Milne, J. Ray, K.D. Devine, and S. Kempka. Operator-split lagrangian-eulerian time integration. *J. Comp. Phys.*, 2000. under review.

[10] H. N. Najm, R. W. Schefer, R. B. Milne, C. J. Mueller, K. D. Devine, and S. N. Kempka. Numerical and experimental investigation of vortical flow-flame interaction. SAND Report SAND98-8232, UC-1409, Sandia National Laboratories, Livermore, CA 94551-0969, February 1998. Unclassified and unlimited release.

[11] S. D. Cohen and A. C. Hindmarsh. Cvode user guide. Technical report UCRL-MA-118618, Lawrence Livermore National Laboratory, Livermore, CA, 1994.

[12] S. D. Cohen and A. C. Hindmarsh. Cvode, a stiff/nonstiff ode solver in c. *Computers in Physics*, 10(2):138–143, 1996.

[13] J. Carrier, L. Greengard, and V. Rokhlin. A fast adaptive multipole algorithm for particle simulations. *SIAM J. Sci Stat. Comput.*, 9:669–686, 1988.

[14] R. W. Bilger, S. H. Starner, and R. J. Kee. *Combustion and Flame*, 80:135–149, 1990.

[15] J. Rehm and P. H. Paul. Reaction rate imaging. *Proc. Combust. Inst.*, 2000. To be published.

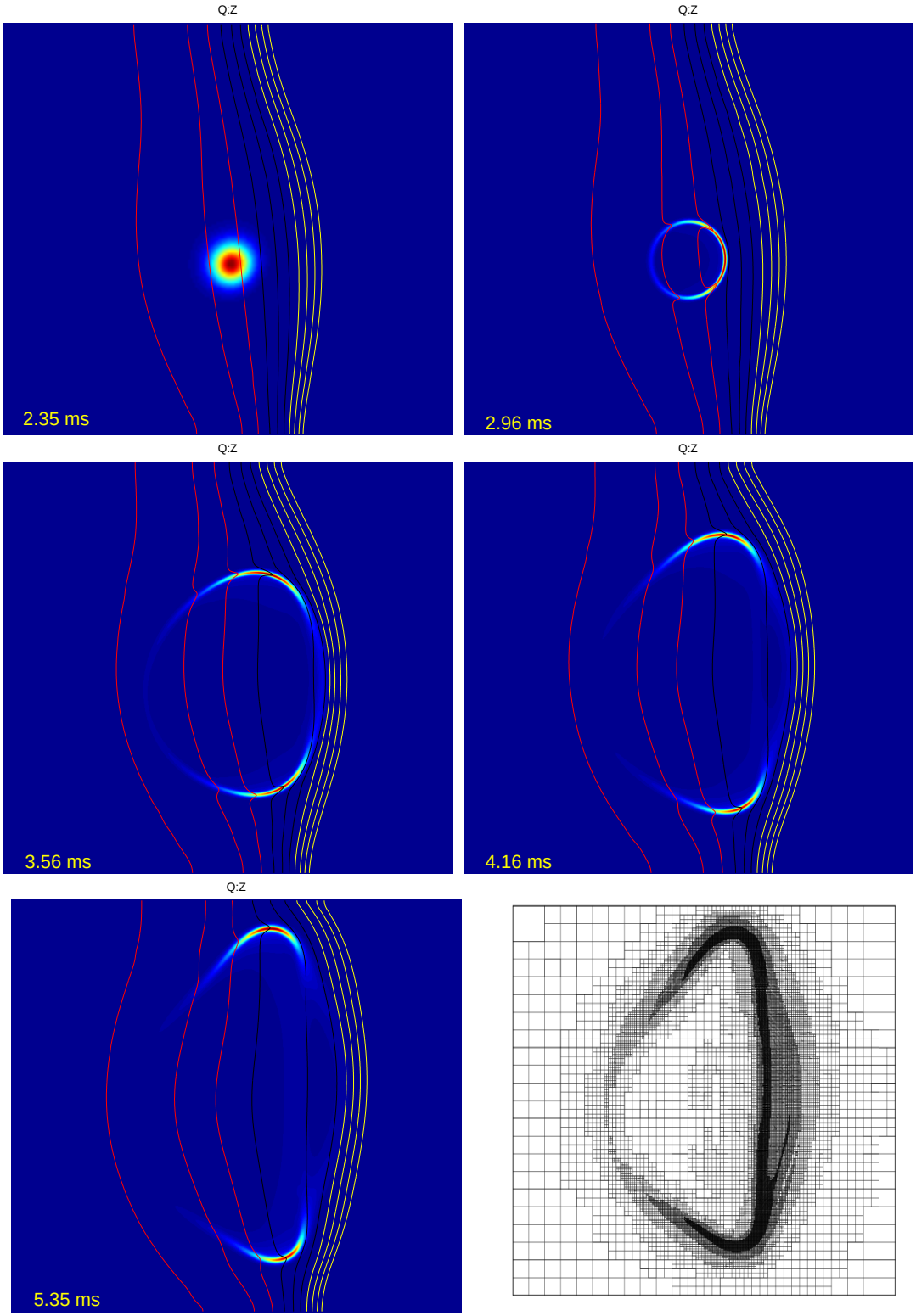

Figure 1: Heat release rate and Z for 5 different time instants. We see a "hot-spot" ignite into two ignition fronts and propagate away along the mixing layer. Only the left half of the domain is shown. The last picture shows the adaptive mesh keeping the premixed kernel resolved. Time is measured from the inception of heating for ignition. Colormap: Blue is mapped to the lowest value, red to the highest.

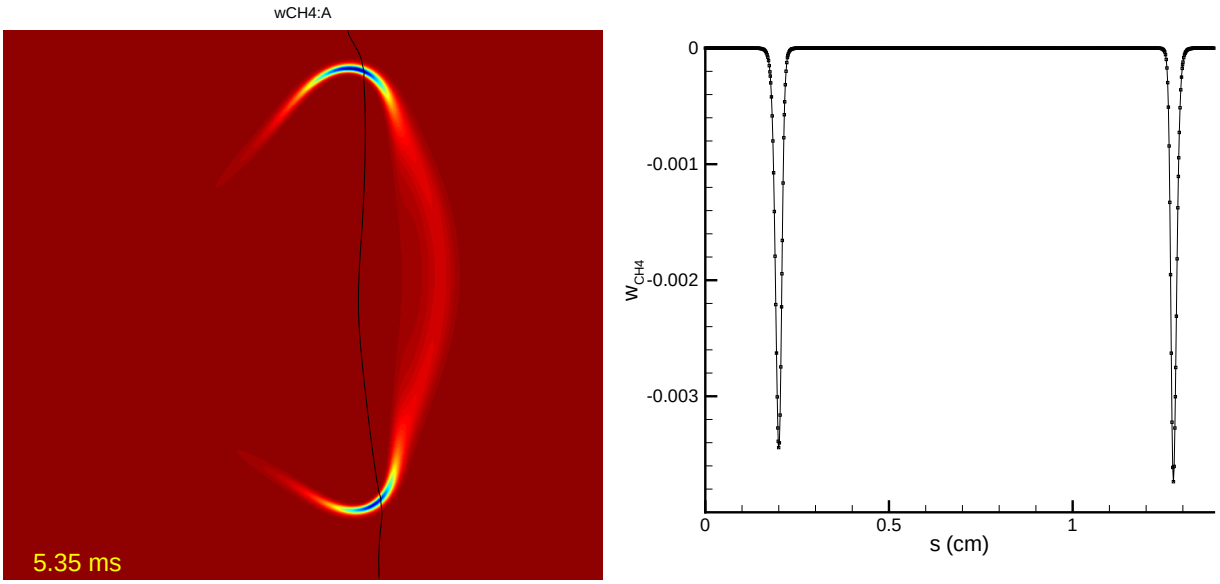

Figure 2: The picture on the left shows the stoichiometric mixture fraction contour passing through the ignition front at t = 5.35 ms as seen in the methane consumption rate colored map. The graph on the right plots the consumption rate of CH_4 along the black contour, by sampling the consumption field. The data points on the graph are plotted with symbols. It is evident that there is a sufficiency of grid points in the ignition fronts. The consumption rate is measured in moles/cm^{2}s. Colormap: Blue is mapped to the lowest value, red to the highest.

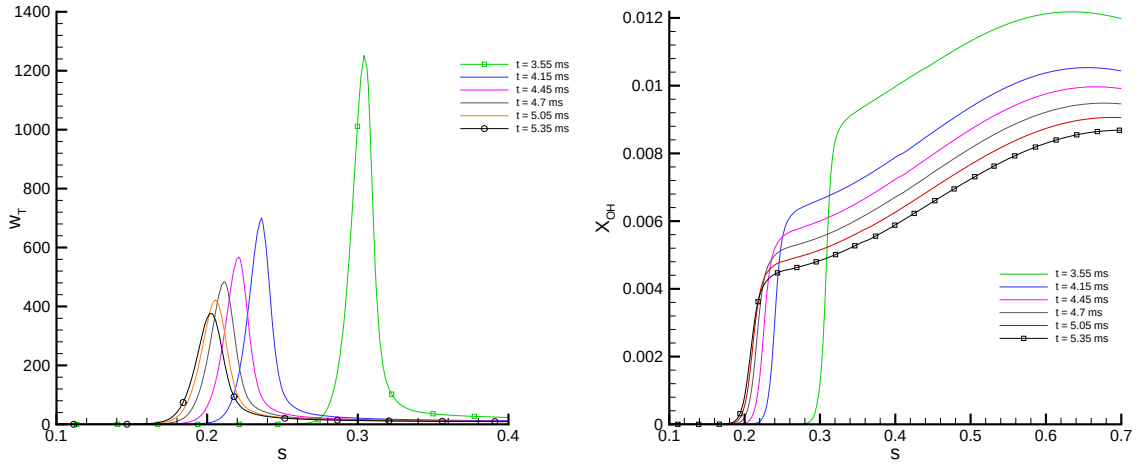

Figure 3: In (a) we plot the heat release rates along the stoichiometric mixture fraction line at different times after ignition for the lower ignition front. The flame is seen to be relaxing and has become almost stationary. The unit for the Y-axis is cal/cm^{2}s and for the X-axis is cm. The maximum heat release rates at those time instants are 1434, 827, 689, 592, 525 and 473 cal/cm^{2}s. In (b) we plot the OH mole fraction. We see remnants from the heating/early ignition phase which are expected to influence the burning in the premixed kernel.

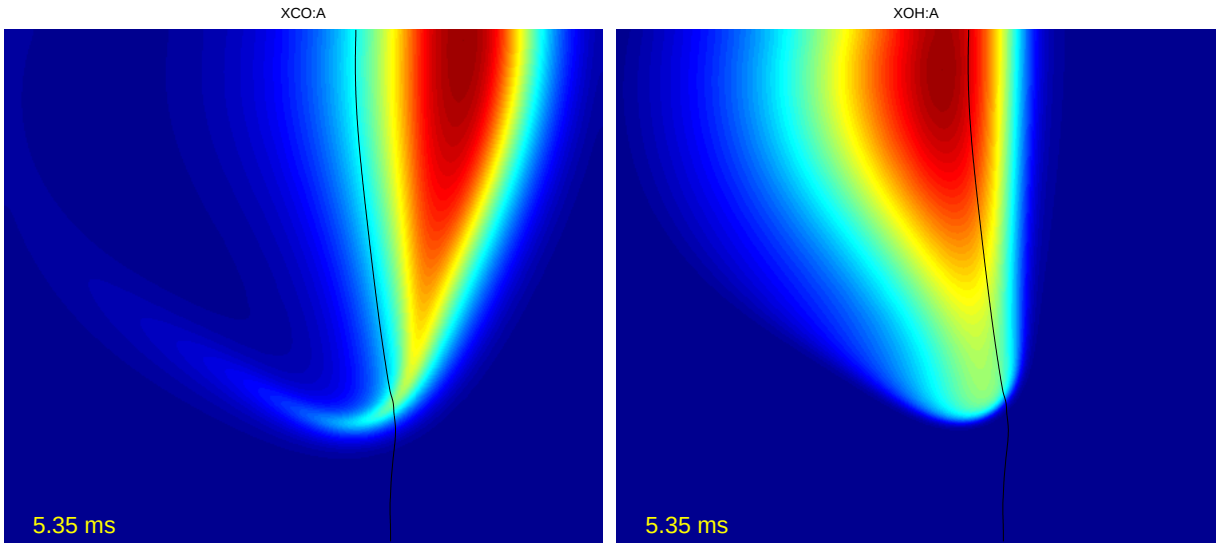

Figure 4: Mole fraction plots of CO (left) and OH (right) at the lower edge flame at $t = 5.35ms$. A "tongue" of OH is surrounded by CO on the rich side of the stoichiometric line, which also curves around the edge into the lean side. Due to the slow recombination reactions of OH most of the OH resides far downstream of the leading edge of the ignition front. The domain shown in the figure has a height of 6.5 mm. Colormap: Blue is mapped to the lowest value, red to the highest.

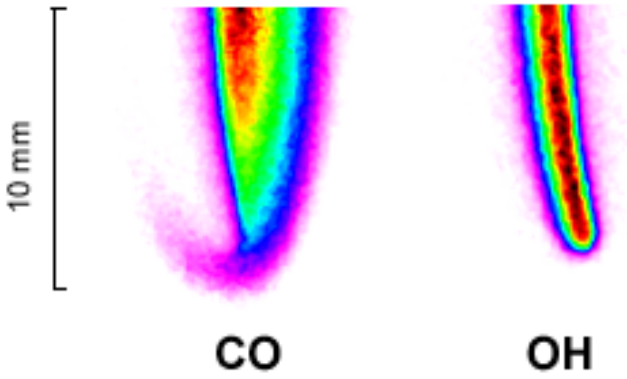

Figure 5: Mole fraction plots of OH and CO at the lower edge of a N_2 diluted methane jet flame. Details of this experiment are in [15]. OH and CO distributions are very similar to those in Fig. 4. Colormap: Blue is mapped to the lowest value, red to the highest. Picture courtesy Jason Rehm, Sandia National Labs., Livermore.

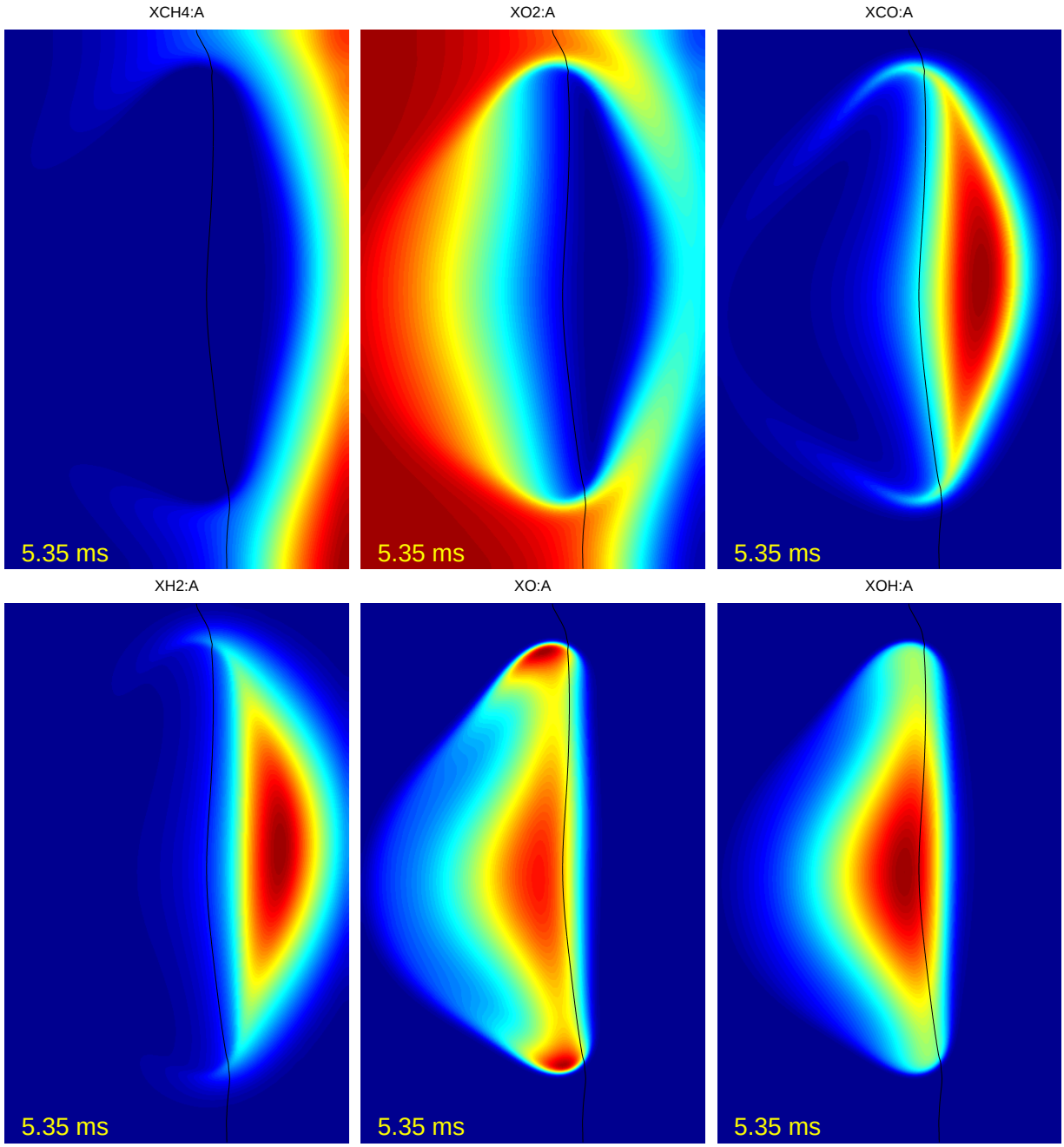

Figure 6: Mole fractions of CH_4, O_2, CO, H_2, O and OH at the lower left ignition front at t = 5.35 ms. Methane is almost entirely consumed at the premixed flame kernel, though O_2 wraps around it. Behind the premixed kernel, the diffusion flame is fueled mainly by CO and H_2 which lie on the rich side and OH and O on the lean side. The black line is the stoichiometric mixture fraction contour. These results are similar to those in [6]. Colormap: Blue is mapped to the lowest value, red to the highest.

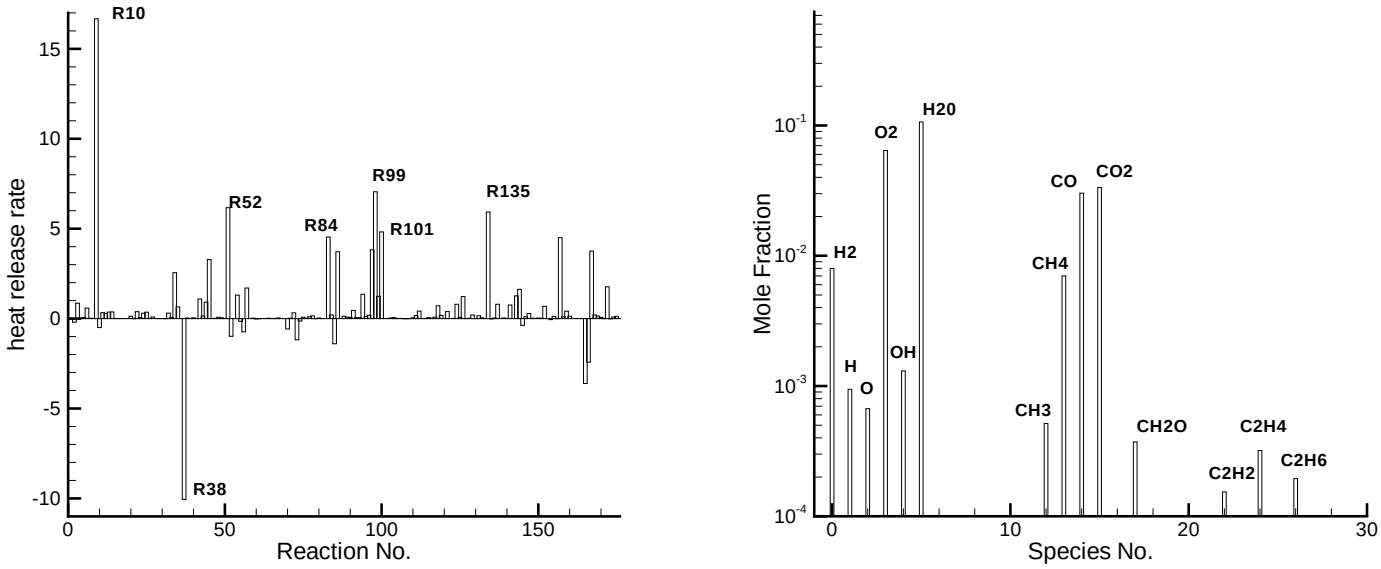

Figure 7: On the left is the contribution to heat release rate by each of the reaction in the premixed kernel, defined as the region where the heat release rate is above 30 cal/cm^{2}s. On the right are the mole fractions of all species. Results presented are averages over the premixed kernel.

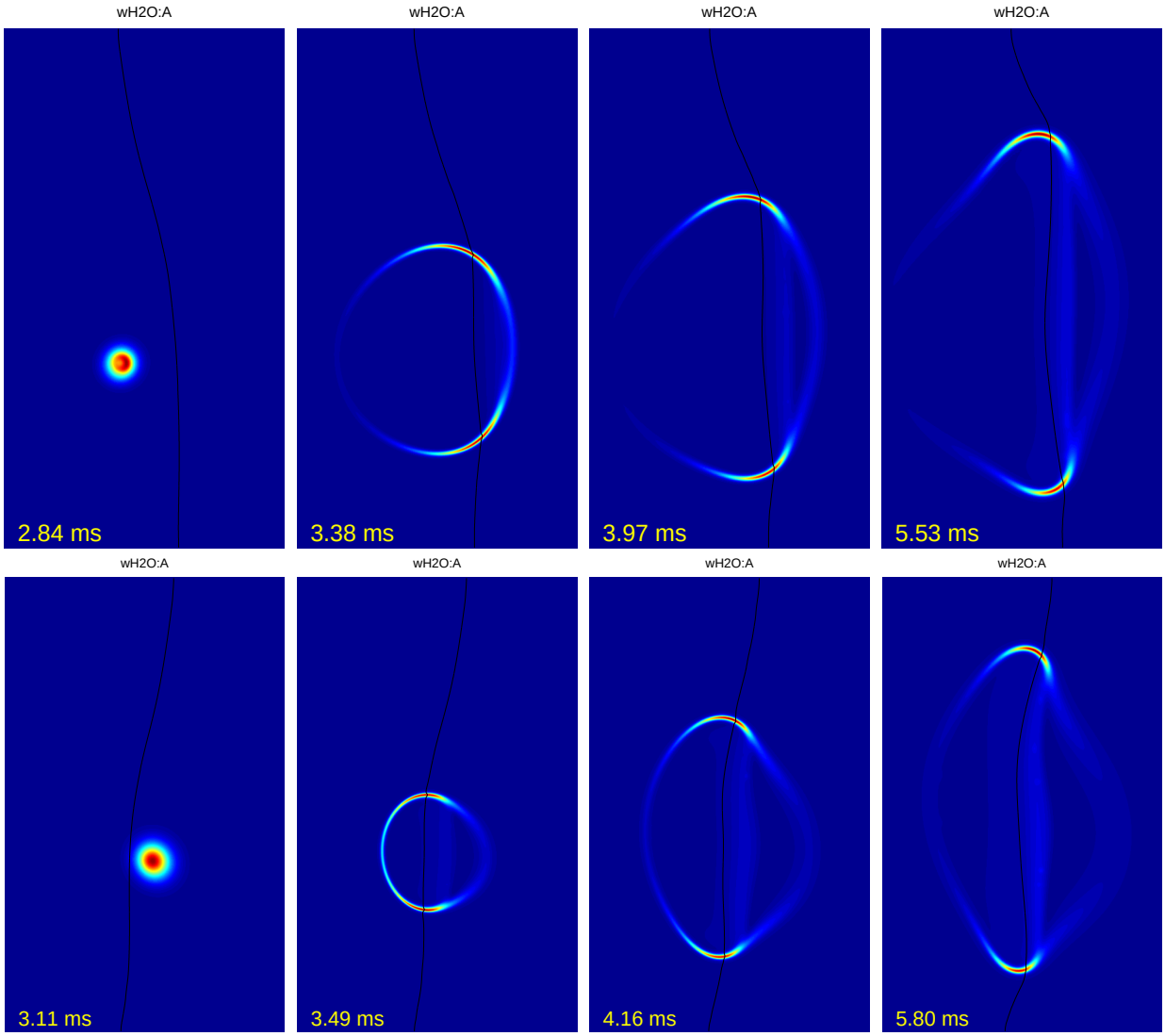

Figure 8: We plot the production rate of H_2O for 2 jet ignition runs. In the first case, (on top) the jet is faster than the coflow (0.8 m/s versus 0.25 m/s); in the second the numbers are reversed. There is a time delay of $\approx$ 30 ms due to the position of the ignition spot with respect to the stoichiometric line (black contour). We see that the development of the ignition fronts is unaffected by the reversal of the strain-rate field. In the second case (bottom), the lean premixed branch has been pushed closer to the stoichiometric line.

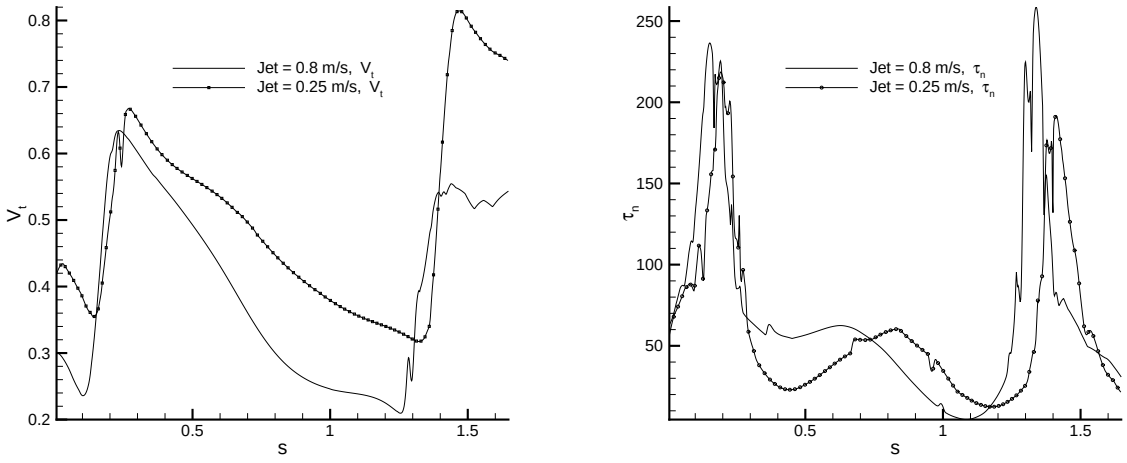

Figure 9: Velocity (left) along and strain-rate (right) normal to the stoichiometric line for t = 5.53 ms (jet velocity = 0.8 m/s) and t = 5.8 ms (jet velocity = 0.25 m/s). The similarity of the two fronts is reflected in the fuel inflow velocities and strain rates. The units for distance s, velocity v_t and strain-rate τ_n are cm, m/s and 1/s.